MOLECULAR AND CELLULAR BIOLOGY, Oct. 2004, p. 8662–8670 Vol. 24, No. 19
0270-7306/04/$08.00+0 DOI: 10.1128/MCB.24.19.8662–8670.2004

Direct Test of Potential Roles of EIIIA and EIIIB Alternatively Spliced Segments of Fibronectin in Physiological and Tumor Angiogenesis

Sophie Astrof,[1] Denise Crowley,[1] Elizabeth L. George,[2]† Tomohiko Fukuda,[3] Kiyotoshi Sekiguchi,[3] Douglas Hanahan,[4] and Richard O. Hynes[1]*

Howard Hughes Medical Institute, Center for Cancer Research, Department of Biology, Massachusetts Institute of Technology, Cambridge,[1] and Vascular Research Division, Department of Pathology, Brigham and Women's Hospital, Boston,[2] Massachusetts; Department of Biochemistry and Biophysics, Comprehensive Cancer Center and Diabetes Center, University of California, San Francisco, San Francisco, California[4]; and Institute for Protein Research, Osaka University, Osaka, Japan[3]

Received 29 April 2004/Returned for modification 26 June 2004/Accepted 13 July 2004

Fibronectin splice variants containing the EIIIA and/or EIIIB exons are prominently expressed in the vasculature of a variety of human tumors but not in normal adult tissues. To understand the functions of these splice variants in physiological and tumor angiogenesis, we used EIIIB-null and EIIIA-null strains of mice to examine neovascularization of mouse retinas, pancreatic tumors in Rip-Tag transgenic mice, and transplanted melanomas. Contrary to expectations, physiological and tumor angiogenesis was not significantly affected by the absence of either EIIIA or EIIIB splice variants. Tumor growth was also not affected. In addition, the expression levels of smooth muscle alpha actin, believed to be modulated by EIIIA-containing fibronectins, were not affected either. Our experiments show that despite their tight regulation during angiogenesis, the presence of EIIIA or EIIIB splice variants individually is not essential for neovascularization.

Angiogenesis is a process whereby new blood vessels develop from the preexisting vasculature (5). This process is crucial to provide oxygen and nutrients to a growing tumor mass; without a vascular supply, tumors fail to grow beyond 1.5 mm in diameter (15, 25). Inhibition of tumor angiogenesis leads to inhibition or retardation of tumor growth in animal tumor models (7). The extracellular milieu plays a prominent role in tumor development by supplying factors that can either enhance (e.g., matrix metalloproteinases [12] or vascular endothelial growth factor [2, 28]) or inhibit (e.g., thrombospondin [48] or tumstatin [23]) tumor growth. Extracellular matrix proteins, including fibronectin (FN) and its splice variants, are prominently expressed in and around tumors (10, 32, 47), but their roles in tumorigenesis are poorly understood. This study investigated the potential functions of FN splice variants, EIIIA and EIIIB, in physiological and tumor angiogenesis.

FN is a large modular glycoprotein composed of type I, type II, and type III FN repeats and implicated in numerous cellular processes from cell migration to hemostasis (27, 39). FN-null embryos and embryoid bodies have very low numbers of endothelial cells and develop defective vessels (16, 18), and FN-null embryos die very early in utero from cardiovascular defects (18–20). These observations underscore the importance of FN in vascular development.

FN RNA is alternatively spliced at three conserved regions, EIIIA (EDA), EIIIB (EDB), and V (CS-1). Although EIIIA and EIIIB sequences are only 29% identical within a species, interspecies comparisons show that amino acid sequences of EIIIB and EIIIA are highly conserved. For example, the mouse and human EIIIB and EIIIA segments are 100% and 96% identical, respectively. The patterns of expression of these splice variants are also conserved among species. In vivo, EIIIA and EIIIB FN splice variants are expressed around developing blood vessels during embryonic growth (14, 21, 44) when vessels are actively forming and being remodeled, but they are markedly downregulated in adult tissues where vascularization is quiescent (43). Nevertheless, EIIIB- and EIIIA-null mice are viable and fertile (17, 38, 57), suggesting that embryonic vessel formation occurs normally in the absence of these splice variants. The animals appear largely normal, although small differences in wound healing, atherosclerosis, and life span have been reported for the EIIIA-null mice (38, 57).

During angiogenesis following vascular injury in an adult, EIIIA and EIIIB FNs become upregulated around blood vessels (30, 55, 56). In addition, FN and its splice variants become highly upregulated around blood vessels in many human tumors (8, 9, 11, 29, 31, 32, 34, 35, 40–42, 46, 52). Indeed, these splice variants are sometimes called "oncofetal fibronectin isoforms" to signify their prominent expression in embryos and tumors (51). Inclusion of the EIIIB exon into FN mRNA has been considered a marker of tumor angiogenesis (9), and high-affinity antibodies that bind to EIIIB$^+$-FN have been shown to localize specifically to tumor vasculature (4, 58).

In vitro and in vivo evidence suggests that EIIIA-FN might play a role in pericyte or smooth muscle cell development. The results of in vitro experiments suggest that EIIIA-FN facilitates transforming growth factor β1 (TGF-β1)-mediated conversion

* Corresponding author. Mailing address: Howard Hughes Medical Institute, Center for Cancer Research, Department of Biology, Massachusetts Institute of Technology, Cambridge, MA 02139. Phone: (617) 253-6422. Fax: (617) 253-8357. E-mail: rohynes@mit.edu.

† Present address: Novartis Institutes for Biomedical Research, Cambridge, MA 02139.

of fibroblastic precursors into myofibroblasts expressing alpha smooth muscle actin (αSMA) (53). In vivo, EIIIA-expressing endothelial cells have been shown to stimulate the conversion of lipocytes into αSMA-expressing myofibroblasts (30). Pericytes share features with myofibroblasts and express αSMA upon maturation (26). Intimate association of pericytes with blood vessel endothelial cells is important for vascular stability and integrity: normal and tumor vessels regress when association between endothelial cells and pericytes is blocked (1, 3).

The high degree of amino acid sequence conservation of EIIIA and EIIIB FNs among species, their tightly regulated vascular pattern of expression, and the data on αSMA induction suggest but do not prove that these splice variants play some important role in angiogenesis. To test this hypothesis, we examined physiological and tumor angiogenesis in mice that lack either EIIIA or EIIIB FNs. Physiological angiogenesis was examined in the context of new vessel growth in the mouse retina, and tumor angiogenesis was examined during pancreatic islet tumorigenesis in Rip1-Tag2 transgenic mice and in a subcutaneous tumor transplant model.

MATERIALS AND METHODS

Animals. All experiments involving animals were approved by Massachusetts Institute of Technology's Committee on Animal Care and were done according to their guidelines ("Interdisciplinary Principles and Guidelines for the Use of Animals in Research, Marketing and Education"). EIIIB-null and EIIIA-null mice were generated in the laboratories of K. Sekiguchi and E. L. George, respectively (17, 57). These mice were crossed with Rip1-Tag2 transgenic mice (24) to generate EIIIB$^{+/-}$ and EIIIB$^{-/-}$ or EIIIA$^{+/-}$ and EIIIA$^{-/-}$ mice heterozygous for simian virus 40 large T-antigen transgene. All mice were of mixed genetic background. EIIIB-RipTag transgenic mice were a mix of 129S4 and C57BL/6J backgrounds, and EIIIA-RipTag mice were of 129S4, C57BL/6J and BALB/c backgrounds. To confirm the absence of EIIIB or EIIIA mRNA in the EIIIB-null or EIIIA-null mice, we performed reverse transcription-PCR (RT-PCR) with RNA isolated from heads of EIIIB$^{+/-}$, EIIIB$^{-/-}$, EIIIA$^{+/-}$ or EIIIA$^{-/-}$ embryos at embryonic day 14.5 using primers 5′-GGGGACCTCTCT GGAAGAAGTGG-3′ and 5′-GTCCCAGGCAGGAGATTTG-3′ for EIIIB or primers 5′-CCCACTGTGGAGTACGTGG-3′ and 5′-GAGTCCTGACACAAT CACCG-3′ for EIIIA.

Retinal angiogenesis. Retinal angiography was performed as described previously (54). Heterozygous and null EIIIB littermates on C57BL/6J background, and heterozygous and null EIIIA littermates (a mix of C57BL/6J and BALB/c strains) were used. Mice were anesthetized with 0.3 g of tribromoethanol 7 days after birth and injected with 200 μl of a solution of fluorescein isothiocyanate (FITC)-dextran (50 mg/ml) (Sigma; molecular weight, 10^6 g/mol) through the heart's left ventricle. Mice were then sacrificed, and retinas were dissected. Five radial cuts were made in each retina for flat mounting on slides. Blood vessels were observed using a Zeiss Axiophot fluorescence microscope. Vessel density was evaluated using OpenLab software as the amount of fluorescence per 100 pixels (three to five areas of 5×10^4 to 10×10^4 pixels covering almost the entire retina were analyzed in each case). Large vessels were excluded from the analysis. At least four retinas of each genotype were analyzed. The box plots were generated using a web-based program (http://alvarez.physics.csbsju.edu/stats/ttest.html). The box represents the interquartile range (IQR, central 50% of the data points), horizontal lines inside the boxes represent the median values, and vertical bars represent a spread of 1.5× IQR, while dots represent outliers, which were included in calculations of significance.

Immunofluorescence. Frozen sections were stained with antibodies to detect PECAM (rat immunoglobulin G) (Pharmingen) (diluted 1:50) and αSMA (FITC-conjugated mouse immunoglobulin G) (Sigma) (diluted 1:100). Rabbit polyclonal antibodies previously generated in our laboratory were used to detect total FN (297.1) or V95+ (73N) FNs (both used at 1:100 dilution) or purified rabbit anti-EIIIB (246) antibody (2.9 μg/ml). Sections were fixed in 4% paraformaldehyde for 10 min and blocked for 30 min with blocking solution that contained phosphate-buffered saline, 10% FN-depleted goat serum, and 0.05% Tween 20 at room temperature. Primary antibodies were mixed together in the blocking solution and incubated with sections at 4°C for 10 h.

To detect EIIIB-containing FN, sections were treated with *N*-glycosidase F (1,800,000 U/mg, diluted 1:20 in G7 buffer [New England Biolabs]) to expose EIIIB epitopes prior to the addition of the primary antibodies for 10 h at 37°C (45). Primary antibodies were detected with Alexa Fluor 594 (red)-conjugated goat anti-rat immunoglobulins and Alexa Fluor 350 (blue)-conjugated goat anti-rabbit immunoglobulins (Molecular Probes) diluted 1:200. When primary antibodies were replaced by normal rat, mouse, or rabbit antibodies, no staining was observed (data not shown). Likewise, no staining was seen when antibodies to EIIIB-FN were used to stain tumor sections derived from EIIIB-null mice (data not shown).

Monoclonal antibody 3E2 (Sigma) and polyclonal goat antibody 153–1 (44) that specifically recognize EIIIA-FN on Western blots produce vascular staining on sections from EIIIA-null mice. In the case of 153–1 antibodies, preincubation with antigenic peptide abolished the staining, indicating that 153–1 recognizes cross-reacting epitopes in EIIIA-null tissues (data not shown).

Isolation of pancreatic islets and tumors. Angiogenic islets and tumors in Rip-Tag transgenic mice were quantified when the animals reached either 12 (EIIIB) or 11 (EIIIA) weeks of age as described previously (15). In brief, type IV collagenase (Worthington; 175 U/mg) was dissolved in RPMI at 2 mg/ml, and 3 ml of this solution were perfused into the pancreas through the bile duct. The pancreas was then removed, placed in a 50-ml Falcon tube, and kept on ice (for up to 1 h). Tubes were then incubated in a 37°C water bath for 21 min, vortexed for 1 min, and reconstituted with 20 ml of RPMI containing 10% fetal bovine serum (FBS). Pancreases were then washed once with 20 ml of RPMI containing 10% FBS by spinning at $200 \times g$. After removing all of the supernatant, pancreata were resuspended in 10 ml of Histopaque-1077 (Sigma) by gentle vortexing and carefully overlaid with 10 ml of RPMI without FBS. The tubes were spun at $913 \times g$ for 30 min, and pancreatic islets and tumors were removed from the interface between Histopaque and RPMI. Islets whose volumes were larger than 1.8 mm^3 (i.e., >1.5 mm in diameter) were counted as tumors. Pink or red islets smaller than 1.8 mm^3 were classified as angiogenic islets (15).

Analysis of subcutaneous tumor growth. EIIIA-null mice on C57BL/6J background and EIIIB-null mice backcrossed into C57BL/6J background for seven generations were used. At 8 weeks of age, EIIIA- or EIIIB-null mice and their heterozygous littermates were injected with 10^5 B16 F_0 mouse melanoma cells into the subcutaneous space of their right flanks. Tumor growth was analyzed 2 weeks later by measuring tumor weight.

RNase protection. DNAs encoding RNA probes were generated by RT-PCR from wild-type skin fibroblasts of newborn mice. The following primers were used to generate the probes for RNase protection: 5′-TGTGAAGAGGAAGA CAGCACAGCC-3′ and 5′-GCAGTGTCGGATGCTCTTCAGG-3′ (αSMA probe, 300 bp), 5′-CCCACTGTGGAGTACGTGG-3′ and 5′-GAGTCCTGAC ACAATCACCG-3′ (EIIIA probe containing 117 bp of the eleventh type III repeat, 270 bp of the EIIIA exon, and 185 bp of the twelfth type III repeat), 5′-GGGGACCTCTCTGGAAGAAGTGG-3′ and 5′-GTCCCAGGCAGGAG ATTTG-3′ (EIIIB probe containing 145 bp of the seventh type III repeat, 273 bp of the EIIIB exon, and 199 bp of the eighth type III repeat), and 5′-GTGTCA CGGAGGCCACCATTACTG-3′ and 5′-GGAACTGTAAGGGCTCTTCGTC G-3′ (V120 probe containing 113 bp of the fourteenth type III repeat, 363 bp of the V120 region, and 128 bp of the fifteenth type III repeat). Tumor RNA was isolated from EIIIB$^{+/-}$, EIIIB$^{-/-}$, EIIIA$^{+/-}$, or EIIIA$^{-/-}$ animals using QIAGEN mini-RNA extraction kit. RNase protection was performed by hybridizing 5 μg of tumor RNA with RNA probes generated by in vitro transcription and labeled with [α-^{32}P]dUTP (6,000 Ci/mmol; New England Nuclear). The reaction mixtures were resolved on 5% polyacrylamide gels containing urea, developed by autoradiography, and quantified with a phosphorimager. Saturating amounts of probe were used, since we did not observe an increase in signal when the amount of probe was doubled (data not shown).

RESULTS

Physiological angiogenesis. EIIIA-null and EIIIB-null mice are viable and fertile, suggesting that angiogenesis in these embryos occurs normally. RT-PCR analysis indicated that EIIIA-null and EIIIB-null embryos indeed lacked EIIIA or EIIIB exons in their FN mRNA (Fig. 1A and B). Furthermore, immunohistochemical analysis showed that EIIIB-null mice lack EIIIB-FN proteins (Fig. 1C and D).

To examine the physiological process of angiogenesis that takes place after birth, we quantified blood vessel growth in the retinas of newborn mice. Mouse retinas, avascular at the time

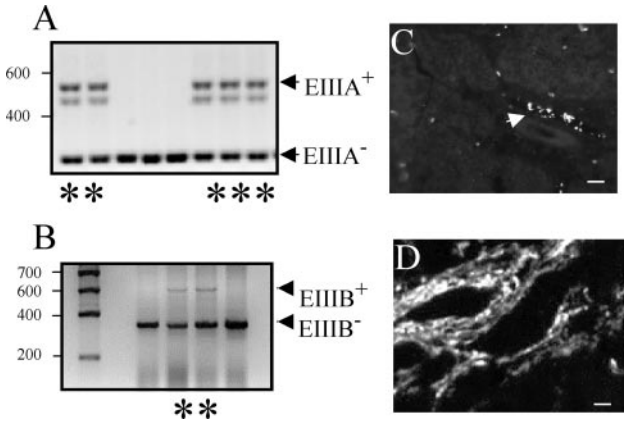

FIG. 1. Expression of EIIIA- and EIIIB-containing FN. (A and B) RT-PCR performed with RNA isolated from heterozygous and null embryos. Lanes with asterisks contain samples taken from heterozygous animals (determined by genomic PCR). RT-PCR performed on mRNA isolated from EIIIA-and EIIIB-null animals shows the absence of these alternatively spliced exons. The positions of molecular size standards (in base pairs) are indicated to the left of the gels. (C) EIIIB-null tumors do not express $EIIIB^+$ proteins. The arrow points to a vessel showing nonspecific staining of red blood cells (45). (D) A tumor section from $EIIIB^{+/-}$ animal stained with antibody to EIIIB showing abundant vascular staining. Bars, 10 μm.

of birth, become vascularized during the first two postnatal weeks (54). The vascularity of mouse retinas was assessed by evaluating the blood vessel density following intracardiac injection of FITC-dextran. We did not observe differences in blood vessel density between littermates of mice that carried heterozygous or homozygous deletion of EIIIB or EIIIA exons (Fig. 2). The median vessel densities in the retinas of animals with EIIIB deletion and EIIIA deletion were 21 and 14.5 fluorescence units per 100 pixels, respectively. This difference in vessel density is probably due to strain-specific genetic factors that influence angiogenic response (22, 49).

Since EIIIA-containing FNs have been implicated in vascular smooth muscle cell differentiation, we examined smooth muscle coverage of tail arteries in cross sections of tails from 7-day-old mice (50). Figure 3 shows that tail arteries from EIIIA- or EIIIB-null mice and those from their heterozygous littermates are enclosed by smooth muscle cells to similar extents. Taken together, these analyses show that the absence of EIIIA or EIIIB exons does not affect the physiological process of angiogenesis in mouse retinas and that the formation of arterial smooth muscle layers is not affected by the absence of EIIIA or EIIIB.

Pathological angiogenesis and expression of FN and its splice variants in murine tumor blood vessels. FN splice variants are highly upregulated in a variety of human tumors. To examine whether FN proteins are similarly upregulated around tumor blood vessels in the Rip1-Tag2 murine tumor model, we stained sections of pancreas containing angiogenic islets and tumors with antibodies recognizing FN and its splice variants. FN is expressed around blood vessels in normal islets (Fig. 4A), but its expression becomes markedly increased around tumor blood vessels (Fig. 4B). Almost coincident with this increase is a massive upregulation of αSMA (Fig. 4 and 5), indicating the appearance of mature pericytes or vascular smooth muscle cells. This upregulation was confirmed by an increase in the number of cells expressing NG2, a different pericyte marker (compare Fig. 5A and B). Pericytes expressing NG2 are present around blood vessels in normal pancreatic islets as well as in tumors (Fig. 5). However, in tumors, NG2+ pericytes are increased in abundance and coexpress αSMA

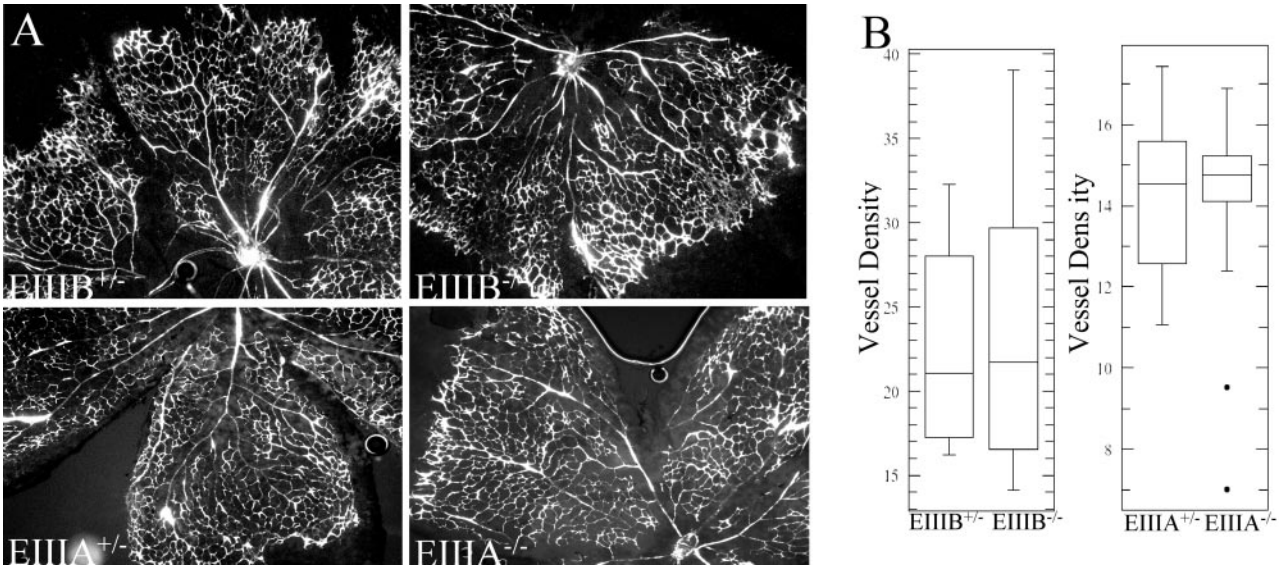

FIG. 2. Physiological blood vessel formation in EIIIA- and EIIIB-null animals. (A) Retinal angiogenesis. Blood vessels, visualized with FITC-dextran, develop normally in EIIIA-null and EIIIB-null animals (right panels) compared with heterozygous littermate controls (left panels). Magnification, ×50. (B) Quantification of vessel density (per 100 pixels). Each data point represents vessel density measured in a 50,000- to 100-thousand pixel area. The difference in the median vessel density between EIIIA and EIIIB strains is probably due to mouse strain-specific factors (see Results). Four retinas were analyzed per genotype, and at least three areas per retina were quantified. See Materials and Methods for the description of the box plot.

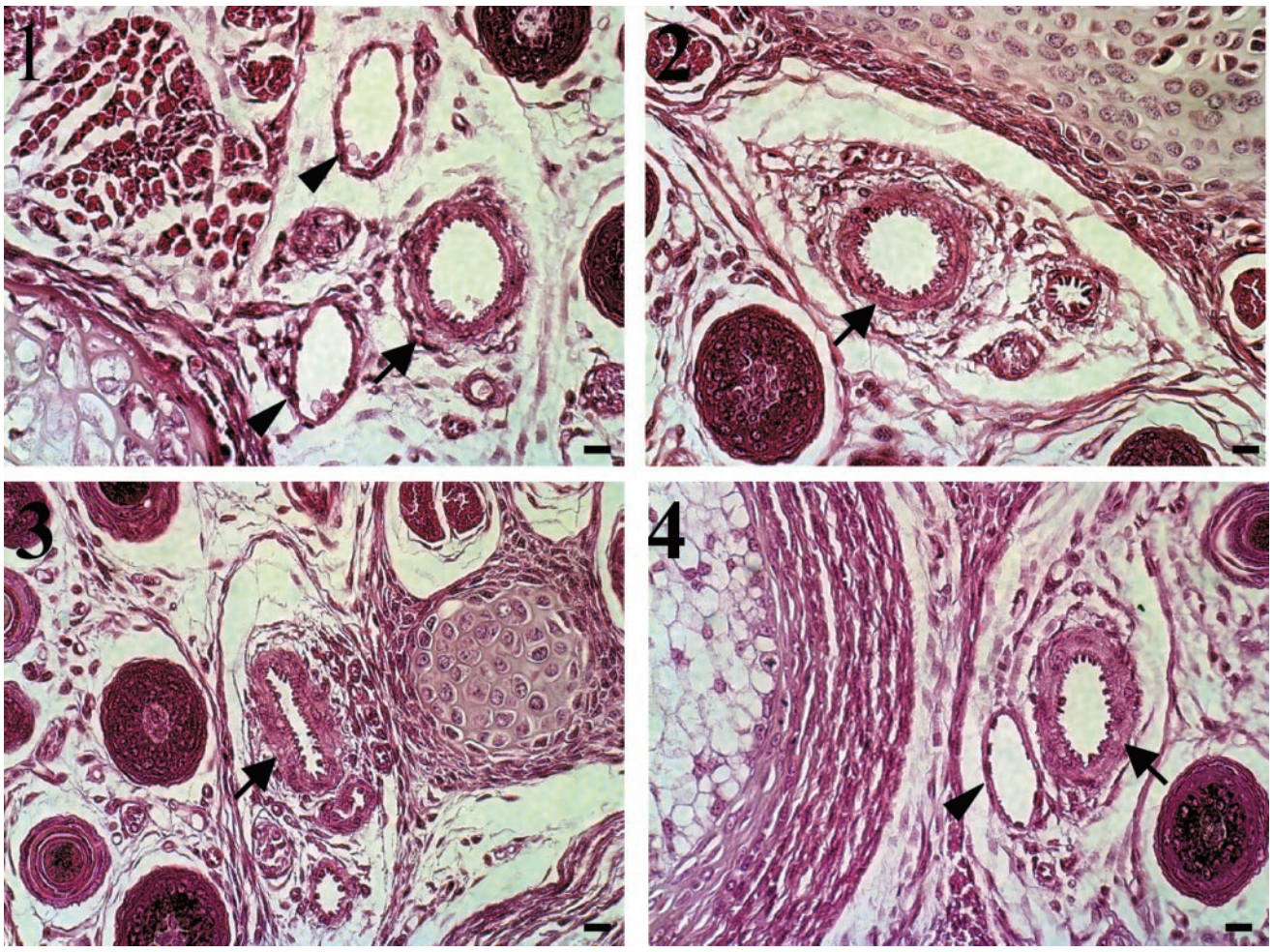

FIG. 3. Tail cross sections from 7-day-old mice were stained with hematoxylin and eosin. Tail sections from EIIIA$^{+/-}$ (panel 1) and EIIIB$^{+/-}$ (panel 3) and EIIIA$^{-/-}$ (panel 2) and EIIIB$^{-/-}$ (panel 4) mice are shown. Arrows point to arteries, and arrowheads point to veins. Bars, 10 μm.

(Fig. 5B). Confocal microscopy showed that tumor pericytes accumulate in the areas between tumor blood vessels, rich in extracellular matrix containing FN and laminin (Fig. 5C and D; also data not shown) as described elsewhere (37).

The expression of EIIIB-FN is also highly upregulated around tumor vasculature. EIIIB-FN is almost nonexistent in the normal pancreas (43; also data not shown) but becomes markedly increased in tumor vessels (Fig. 5D). Upregulation of

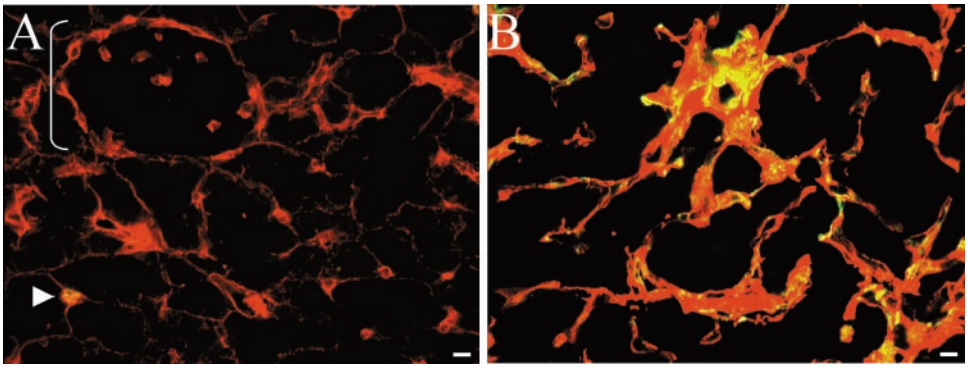

FIG. 4. Tumor blood vessels markedly upregulate FN and αSMA. (A) Normal pancreatic islet (bracket) surrounded by exocrine tissue. Cells were stained to detect FN (red) and αSMA (green), and the overlap between the two is shown in yellow. Note that in normal tissue, expression of αSMA could be found only around arterioles (arrowhead). (B) A tumor section from a Rip-Tag transgenic mouse, wild type for FN. Both FN and αSMA are highly upregulated around the tumor vasculature. Bars, 10 μm.

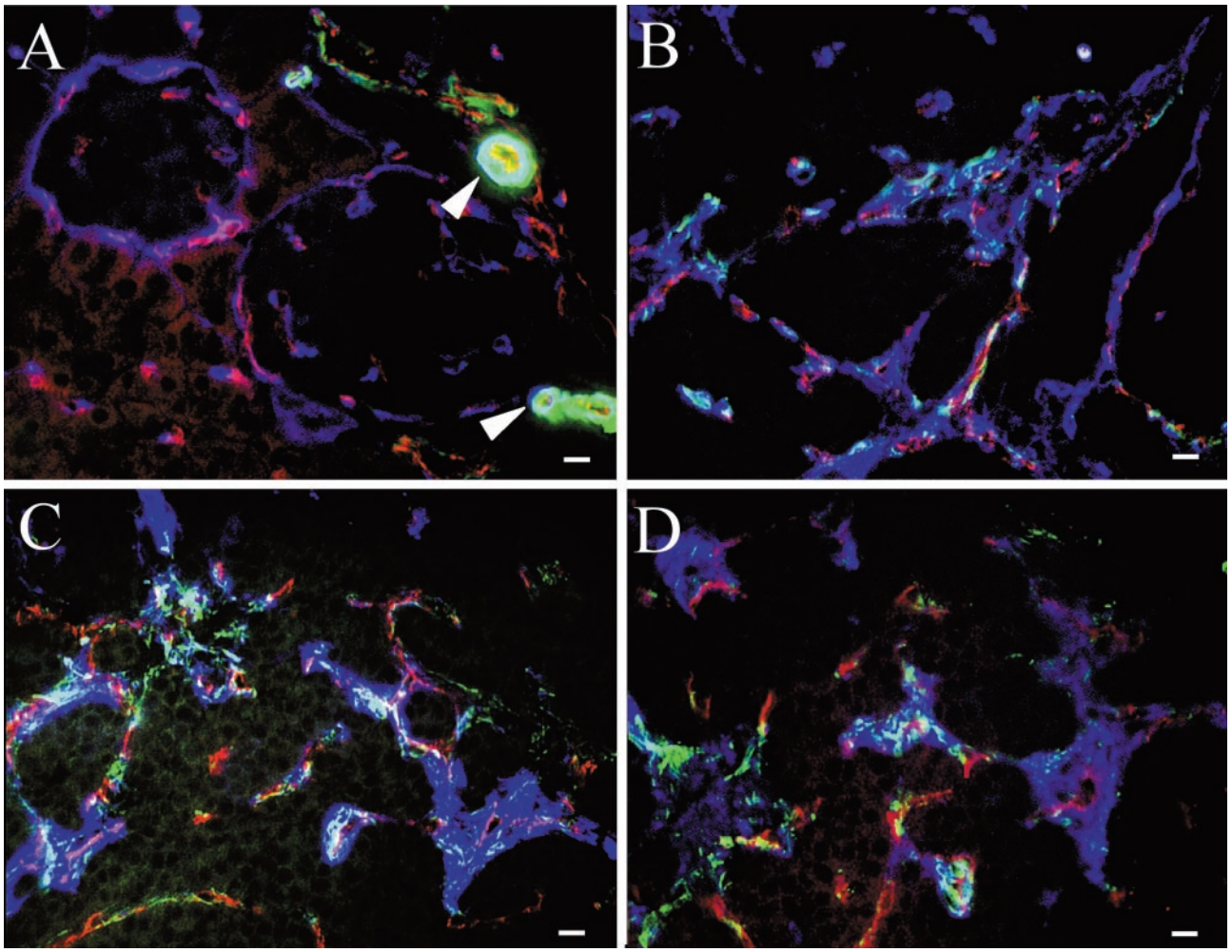

FIG. 5. Expression of FN and splice variants in tumor blood vessels. In all panels, endothelial cells were stained to detect PECAM1 (red), smooth muscle cells are stained to detect αSMA (green), and NG2 (blue in panels A and B) or FNs (blue in panels C and D). (A) Wild-type pancreatic tissue. αSMA expression (green) is seen only around arterioles (arrowheads) near normal pancreatic islets. Small blood vessels express NG2 (blue) but not αSMA (green). (B to D) Rip-Tag tumors. Tumor blood vessels upregulate NG2 (blue) (B) and FN splice variantsV95 (blue) (C) and EIIIB (blue) (D), as well as αSMA (green) (B to D). Bars, 10 μm.

EIIIB also coincides with the increase in the numbers of cells expressing NG2 and αSMA (Fig. 5B). EIIIA-FN mRNA is also expressed in tumors as determined from RNase protection experiments (Fig. 7A). Taken together, these studies demonstrated that, as in human tumors, FN and its splice variants are upregulated around tumor vasculature in mice.

Angiogenesis and tumorigenesis in EIIIA-null and EIIIB-null mice. To examine the roles of EIIIA- and EIIIB-FN in tumor angiogenesis, we used the Rip1-Tag2 transgenic mouse model, wherein islet cell carcinomas develop in the pancreas via a multistage pathway. In this model, neoplastic angiogenesis can be assessed quantitatively by determining the numbers of pancreatic islets that have undergone an angiogenic switch (15). Despite the tight regulation of EIIIB and EIIIA expression during neoplastic transformation, the numbers of angiogenic islets in EIIIB-null and heterozygous mice and in EIIIA-null or heterozygous animals were not statistically different (Fig. 6A and C). Tumor progression, assessed by measuring the numbers of tumors and their size, was also unaffected by the absence of EIIIB- or EIIIA-containing splice variants (Fig. 6B and D).

To address the possibility that other FN splice variants might have been upregulated to compensate for the absence of either EIIIA or EIIIB, we performed RNase protection analysis of tumors derived from EIIIA-null or EIIIB-null animals. These experiments showed that RNA levels of other splice variants of FN were not changed in the absence of EIIIA or EIIIB (Fig. 7 and Table 1). Taken together, the results of our studies indicate that the individual absence of EIIIA- or EIIIB-FN splice variants does not significantly affect tumor angiogenesis or tumor growth in Rip1-Tag2 transgenic mice.

The results of previous in vitro and in vivo studies suggested that αSMA becomes upregulated in pericyte precursors stimulated with EIIIA-FN. To address whether EIIIA-FN is required to induce αSMA expression, we analyzed αSMA expression in EIIIA-null tumors by immunofluorescence (Fig. 8) and quantified the levels of αSMA mRNA by RNase protection (Table 1). Both immunofluorescence and RNase protec-

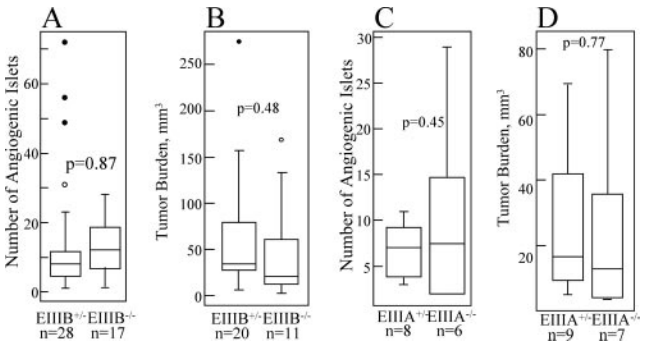

FIG. 6. Islet tumorigenesis in the absence of EIIIB- or EIIIA-FN. (A) EIIIB$^{-/-}$ and EIIIB$^{+/-}$ Rip-Tag transgenic mice. The numbers of angiogenic islets isolated from 12-week-old Rip-Tag transgenic mice are shown (n is the number of animals used). (B) Tumor burden at 12 weeks of age. Tumor burden per mouse is the sum of volumes of all tumors in a mouse. (C) EIIIA$^{-/-}$ and EIIIA$^{-/+}$ Rip-Tag transgenic mice. The numbers of angiogenic islets isolated from 11-week-old transgenic mice are shown. (D) Tumor burden at 11 weeks of age. Tumor burden was also assessed in 13-week-old animals on the mixed background, as well as in animals bred onto the BALB/c genetic background. Three independent experiments showed no statistically significant differences in the extent of the tumor growth between EIIIA$^{-/-}$ and EIIIA$^{+/-}$ animals (data not shown). Data from one experiment are shown. In this figure, *P* is the probability that the null hypothesis is true, as calculated by a two-tailed Student's *t* test. *P* values calculated according to the Wilcoxon sum-of-ranks test were 0.15, 0.12, 0.93, and 0.35 for panels A, B, C, and D, respectively. See Materials and Methods for information on the method used to generate the box plot.

tion experiments showed that αSMA is expressed in pericytes around blood vessels in EIIIA-null and EIIIB-null tumors and that the amount of αSMA mRNA was not affected by the absence of either EIIIA or EIIIB.

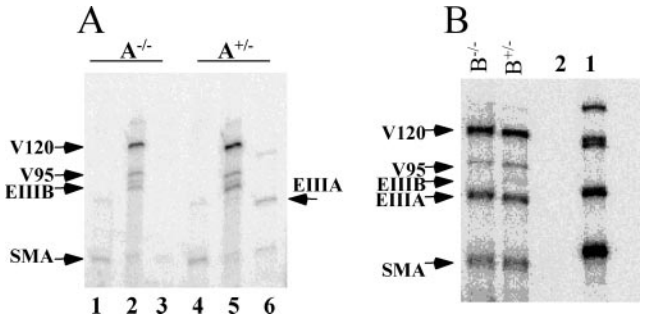

FIG. 7. Quantification of mRNA levels of FN splice variants in islet tumors isolated from EIIIA- or EIIIB-null animals. (A) RNase protection analysis of EIIIA-null and heterozygous tumors from Rip-Tag animals. Lanes 1 and 4 show the bands protected with the αSMA probe, lanes 2 and 5 show the bands protected with the V120 and EIIIB probes, and lanes 3 and 6 show the bands protected with the EIIIA probe. Results of quantification relative to the intensity of β-actin band are presented in Table 1. (B) RNase protection analysis of EIIIB-null and heterozygous tumors. Lane 1 contains undigested probes (V120, EIIIB, EIIIA, and αSMA). These four probes were used simultaneously for RNase protection. Lane 2 shows control hybridization using *Saccharomyces cerevisiae* RNA. In samples from EIIIB$^{+/-}$ and EIIIB$^{-/-}$ tumors, arrows point to V120-, V95-, EIIIB-, EIIIA-, and αSMA-protected bands. Results of quantification relative to the intensity of β-actin band are presented in Table 1.

TABLE 1. Quantification of FN splice variants in tumors isolated from EIIIA- or EIIIB-null animals

Mice	Relative RNA level[a]			
	SMA	EIIIB	EIIIA	V120
EIIIA$^{+/-}$	14.9	142.9, 101.8		253.3, 81.6
EIIIA$^{-/-}$	13.9, 16.4	121.1, 114.5		215.1, 118.3
EIIIB$^{+/-}$	1,564 ± 720		1,050 ± 470	2,064 ± 819
EIIIB$^{-/-}$	1,339 ± 263		820 ± 472	1,507 ± 594

[a] FN and αSMA RNA levels from EIIIA- or EIIIB-null and EIIIA or EIIIB heterozygous tumors. Intensities of the bands are relative to the intensity of the β-actin band. The values for EIIIA$^{+/-}$ and EIIIA$^{-/-}$ mice are from two independent experiments (except for the single value given for SMA RNA in EIIIA$^{+/-}$ mice). The values for EIIIB$^{+/-}$ and EIIIB$^{-/-}$ mice are the means ± standard errors of the means from four independent experiments.

Growth of subcutaneous tumors in EIIIA- and EIIIB-null mice. Gene knockout and cell biology experiments have shown that vessel growth may be affected by distinct players in different tissues (13, 36). Therefore, we investigated whether the absence of EIIIA- or EIIIB-FN splice variants might play a role in tumors grown in a different site, under the skin. B16 mouse melanoma cells were injected into the subcutaneous space of EIIIB- or EIIIA-null mice that had been backcrossed with C57BL/6J mice, and tumor weight was assayed 2 weeks later. B16 cells grown in tissue culture include EIIIA but not EIIIB into their FN mRNA (data not shown). Analysis of tumor weights indicated that there were no differences in tumors grown in EIIIB- or EIIIA-null or their heterozygous littermates (Fig. 9). Taken together, our studies indicated that individually, the absence of EIIIA or EIIIB splice variants of FN does not significantly affect the process of tumor vascularization or tumor progression in either the Rip1-Tag2 or subcutaneous tumor models.

DISCUSSION

The functions of EIIIA and EIIIB splice variants of FN have eluded researchers for almost a decade. The high sequence identity and conserved expression pattern that correlates with newly forming blood vessels suggested that EIIIA and EIIIB splice variants of FN might function in vascular development. Since the absence of either exon does not affect vessel growth during embryogenesis, we examined the roles of these splice variants in physiological angiogenesis after birth and in tumor angiogenesis.

We found that physiological angiogenesis, such as vascularization of retinas in newborn mice, was not affected by the absence of either EIIIA or EIIIB. Similarly, tumor angiogenesis and tumor growth were not affected either. We examined two types of tumor: pancreatic tumors spontaneously arising due to the expression of simian virus 40 large T-antigen transgene in the pancreatic islet β cells and subcutaneous tumors derived from injected B16 mouse melanoma cells. Both types of tumor grew equally well in EIIIA-null and EIIIB-null mice compared to their heterozygous littermates. We also found that the expression of other FN splice variants in the pancreatic islet tumors was unaltered when EIIIA or EIIIB sequences were deleted.

The lack of significant effect on angiogenesis in the EIIIA or EIIIB knockout mice was unexpected, since there is a large

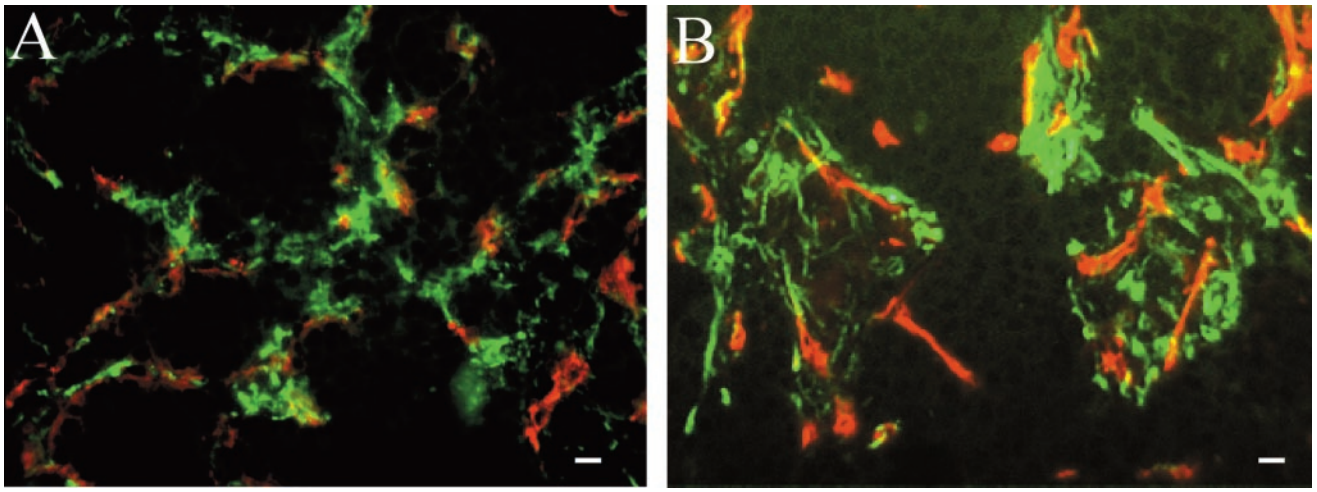

FIG. 8. Tumor vessel pericytes in EIIIA- and EIIIB-null Rip-Tag animals express αSMA. Frozen tumor sections were stained with antibodies to PECAM1 (red) and αSMA (green), and the overlap between the two is shown in yellow. (A) EIIIA-null tumor section. (B) EIIIB-null tumor section. Bars, 10 μm.

body of published data describing the upregulation of these splice variants around angiogenic and tumor blood vessels (see introduction).

It is important to note that the correlation of expression of EIIIA and EIIIB FN splice variants with angiogenesis does not unequivocally prove that they are required for angiogenesis to take place. Only the analyses of mice lacking either of these two exons (17, 38, 57; this study) provide a direct test of functional relevance of these segments for in vivo angiogenesis and tumor growth. These analyses show clearly that individually, neither of the splice variants is necessary for these processes.

Interestingly, EIIIA-null and EIIIB-null tumor vessels still contained cells expressing αSMA, and the levels of αSMA were the same in null and heterozygous animals. Arteries in the mouse tails from null and heterozygous animals in this study were also surrounded by smooth muscle layers to a similar extent. These results were unexpected, because the results of some in vitro experiments had suggested that EIIIA-FN might be necessary to induce αSMA expression, since antibodies to EIIIA abolished TGFβ1-mediated expression of αSMA in myofibroblasts (53). Our results suggest that neither EIIIA nor EIIIB is required for αSMA induction. However, it remains possible that growth factors other than TGFβ1 may induce αSMA expression in the absence of EIIIA or EIIIB.

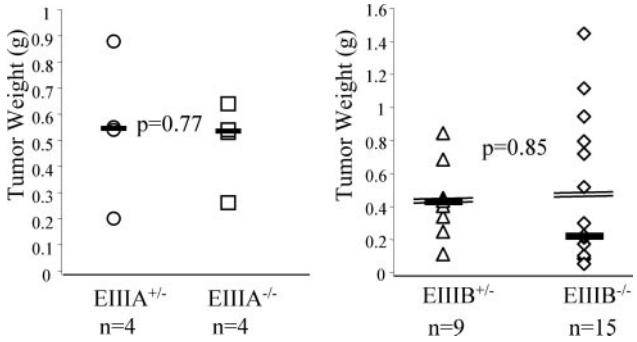

FIG. 9. Growth of subcutaneous B16 tumors in EIIIA- and EIIIB-null mice. B16 F_0 tumor cells were injected subcutaneously into EIIIA-null or EIIIB-null or heterozygous mice at 8 weeks of age. Tumors were collected after 14 (EIIIA) or 17 (EIIIB) days. Medians (solid horizontal lines) and means (double lines) (EIIIB) are indicated. *P* values were calculated by the two-tailed Student's *t* test. Histological sections also showed no visible differences in tumors grown in null and heterozygous animals (data not shown).

Through the millions of years of evolution, the amino acid sequences of EIIIA and EIIIB alternatively spliced exons remained highly conserved, strongly implying their functional importance. Structural studies suggested that each consecutive module of FN may introduce a rotation in the FN molecule (33). Inclusion or exclusion of each alternatively spliced exon might therefore modulate the structure and function of FN. For example, inclusion of EIIIB into FN protein causes unmasking of some epitopes and disappearance of others (6). In addition, mouse embryo fibroblasts carrying a deletion of EIIIB exon are somewhat defective in their ability to assemble cell surface fibrils containing FN and have a cell growth defect (17). However, it is possible that in vivo, the absence of EIIIA splice variant is compensated by the presence of EIIIB and vice versa. If this is the case, simultaneous targeted deletion of both of these splice variants may be necessary to understand their function.

ACKNOWLEDGMENTS

We thank Jing Ye and Juliana Brown for demonstrating isolation of pancreatic islets and the laboratory of Morris White for the islet isolation protocol. We thank J. Fidler for providing B16 F_0 mouse melanoma cells, Heather Moher and Mary Connolly for help with genotyping, and Kris Hewes for demonstrating intracardiac injections. We are grateful to Daniela Taverna and other members of the Hynes laboratory for helpful suggestions throughout the duration of this work and Arjan van der Flier, Lei Xu, Joe McCarty, and Nathan Astrof for critical reading of the manuscript.

This work was supported in part by grants from the NIH (1-PO1-HL66105-03) and the Howard Hughes Medical Institute, in which R.O.H. is an Investigator. S.A. was supported by postdoctoral fellowship grant PF-01-146-01-CSM from the American Cancer Society.

REFERENCES

1. **Benjamin, L. E., I. Hemo, and E. Keshet.** 1998. A plasticity window for blood vessel remodelling is defined by pericyte coverage of the preformed endothelial network and is regulated by PDGF-B and VEGF. Development **125:**1591–1598.
2. **Benjamin, L. E., and E. Keshet.** 1997. Conditional switching of vascular endothelial growth factor (VEGF) expression in tumors: induction of endothelial cell shedding and regression of hemangioblastoma-like vessels by VEGF withdrawal. Proc. Natl. Acad. Sci. USA **94:**8761–8766.
3. **Bergers, G., S. Song, N. Meyer-Morse, E. Bergsland, and D. Hanahan.** 2003. Benefits of targeting both pericytes and endothelial cells in the tumor vasculature with kinase inhibitors. J. Clin. Investig. **111:**1287–1295.
4. **Borsi, L., E. Balza, M. Bestagno, P. Castellani, B. Carnemolla, A. Biro, A. Leprini, J. Sepulveda, O. Burrone, D. Neri, and L. Zardi.** 2002. Selective targeting of tumoral vasculature: comparison of different formats of an antibody (L19) to the ED-B domain of fibronectin. Int. J. Cancer **102:**75–85.
5. **Carmeliet, P.** 2000. Mechanisms of angiogenesis and arteriogenesis. Nat. Med. **6:**389–395.
6. **Carnemolla, B., A. Leprini, G. Allemanni, M. Saginati, and L. Zardi.** 1992. The inclusion of the type III repeat ED-B in the fibronectin molecule generates conformational modifications that unmask a cryptic sequence. J. Biol. Chem. **267:**24689–24692.
7. **Carpizo, D., and M. L. Iruela-Arispe.** 2000. Endogenous regulators of angiogenesis—emphasis on proteins with thrombospondin-type I motifs. Cancer Metastasis Rev. **19:**159–165.
8. **Castellani, P., L. Borsi, B. Carnemolla, A. Biro, A. Dorcaratto, G. L. Viale, D. Neri, and L. Zardi.** 2002. Differentiation between high- and low-grade astrocytoma using a human recombinant antibody to the extra domain-B of fibronectin. Am. J. Pathol. **161:**1695–1700.
9. **Castellani, P., G. Viale, A. Dorcaratto, G. Nicolo, J. Kaczmarek, G. Querze, and L. Zardi.** 1994. The fibronectin isoform containing the ED-B oncofetal domain: a marker of angiogenesis. Int. J. Cancer **59:**612–618.
10. **Clark, E. A., T. R. Golub, E. S. Lander, and R. O. Hynes.** 2000. Genomic analysis of metastasis reveals an essential role for RhoC. Nature **406:**532–535.
11. **D'Ovidio, M. C., A. Mastracchio, A. Marzullo, M. Ciabatta, B. Pini, S. Uccini, L. Zardi, and L. P. Ruco.** 1998. Intratumoral microvessel density and expression of ED-A/ED-B sequences of fibronectin in breast carcinoma. Eur. J. Cancer **34:**1081–1085.
12. **Egeblad, M., and Z. Werb.** 2002. New functions for the matrix metalloproteinases in cancer progression. Nat. Rev. Cancer **2:**161–174.
13. **Ferrara, N., J. Lecouter, and R. Lin.** 2002. Endocrine gland vascular endothelial growth factor (EG-VEGF) and the hypothesis of tissue-specific regulation of angiogenesis. Endocr. Res. **28:**763–764.
14. **Ffrench-Constant, C., and R. O. Hynes.** 1989. Alternative splicing of fibronectin is temporally and spatially regulated in the chicken embryo. Development **106:**375–388.
15. **Folkman, J., K. Watson, D. Ingber, and D. Hanahan.** 1989. Induction of angiogenesis during the transition from hyperplasia to neoplasia. Nature **339:**58–61.
16. **Francis, S. E., K. L. Goh, K. Hodivala-Dilke, B. L. Bader, M. Stark, D. Davidson, and R. O. Hynes.** 2002. Central roles of α5β1 integrin and fibronectin in vascular development in mouse embryos and embryoid bodies. Arterioscler. Thromb. Vasc. Biol. **22:**927–933.
17. **Fukuda, T., N. Yoshida, Y. Kataoka, R. Manabe, Y. Mizuno-Horikawa, M. Sato, K. Kuriyama, N. Yasui, and K. Sekiguchi.** 2002. Mice lacking the EDB segment of fibronectin develop normally but exhibit reduced cell growth and fibronectin matrix assembly in vitro. Cancer Res. **62:**5603–5610.
18. **George, E. L., H. S. Baldwin, and R. O. Hynes.** 1997. Fibronectins are essential for heart and blood vessel morphogenesis but are dispensable for initial specification of precursor cells. Blood **90:**3073–3081.
19. **George, E. L., and R. O. Hynes.** 1994. Gene targeting and generation of mutant mice for studies of cell-extracellular matrix interactions. Methods Enzymol. **245:**386–420.
20. **Georges-Labouesse, E. N., E. L. George, H. Rayburn, and R. O. Hynes.** 1996. Mesodermal development in mouse embryos mutant for fibronectin. Dev. Dyn. **207:**145–156.
21. **Glukhova, M. A., M. G. Frid, B. V. Shekhonin, Y. V. Balabanov, and V. E. Koteliansky.** 1990. Expression of fibronectin variants in vascular and visceral smooth muscle cells in development. Dev. Biol. **141:**193–202.
22. **Gupta, A. R., N. S. Dejneka, R. J. D'Amato, Z. Yang, N. Syed, A. M. Maguire, and J. Bennett.** 2001. Strain-dependent anterior segment neovascularization following intravitreal gene transfer of basic fibroblast growth factor (bFGF). J. Gene Med. **3:**252–259.
23. **Hamano, Y., M. Zeisberg, H. Sugimoto, J. C. Lively, Y. Maeshima, C. Yang, R. O. Hynes, Z. Werb, A. Sudhakar, and R. Kalluri.** 2003. Physiological levels of tumstatin, a fragment of collagen IV α3 chain, are generated by MMP-9 proteolysis and suppress angiogenesis via αVβ3 integrin. Cancer Cell **3:**589–601.
24. **Hanahan, D.** 1985. Heritable formation of pancreatic beta-cell tumours in transgenic mice expressing recombinant insulin/simian virus 40 oncogenes. Nature **315:**115–122.
25. **Hanahan, D., and R. A. Weinberg.** 2000. The hallmarks of cancer. Cell **100:**57–70.
26. **Hirschi, K. K., S. A. Rohovsky, and P. A. D'Amore.** 1998. PDGF, TGF-beta, and heterotypic cell-cell interactions mediate endothelial cell-induced recruitment of 10T1/2 cells and their differentiation to a smooth muscle fate. J. Cell Biol. **141:**805–814.
27. **Hynes, R. O.** 1990. Fibronectins. Springer-Verlag, New York, N.Y.
28. **Inoue, M., J. H. Hager, N. Ferrara, H. P. Gerber, and D. Hanahan.** 2002. VEGF-A has a critical, nonredundant role in angiogenic switching and pancreatic beta cell carcinogenesis. Cancer Cell **1:**193–202.
29. **Inufusa, H., M. Nakamura, T. Adachi, Y. Nakatani, K. Shindo, M. Yasutomi, and H. Matsuura.** 1995. Localization of oncofetal and normal fibronectin in colorectal cancer. Correlation with histologic grade, liver metastasis, and prognosis. Cancer **75:**2802–2808.
30. **Jarnagin, W. R., D. C. Rockey, V. E. Koteliansky, S. S. Wang, and D. M. Bissell.** 1994. Expression of variant fibronectins in wound healing: cellular source and biological activity of the EIIIA segment in rat hepatic fibrogenesis. J. Cell Biol. **127:**2037–2048.
31. **Kaczmarek, J., P. Castellani, G. Nicolo, B. Spina, G. Allemanni, and L. Zardi.** 1994. Distribution of oncofetal fibronectin isoforms in normal, hyperplastic and neoplastic human breast tissues. Int. J. Cancer **59:**11–16.
32. **Kosmehl, H., A. Berndt, S. Strassburger, L. Borsi, P. Rousselle, U. Mandel, P. Hyckel, L. Zardi, and D. Katenkamp.** 1999. Distribution of laminin and fibronectin isoforms in oral mucosa and oral squamous cell carcinoma. Br. J. Cancer **81:**1071–1079.
33. **Leahy, D. J., I. Aukhil, and H. P. Erickson.** 1996. 2.0 A crystal structure of a four-domain segment of human fibronectin encompassing the RGD loop and synergy region. Cell **84:**155–164.
34. **Lohi, J., T. Tani, L. Laitinen, L. Kangas, V. P. Lehto, and I. Virtanen.** 1995. Tenascin and fibronectin isoforms in human renal cell carcinomas, renal cell carcinoma cell lines and xenografts in nude mice. Int. J. Cancer **63:**442–449.
35. **Matsumoto, E., T. Yamada, Y. Kawarada, and T. Sakakuro.** 1999. Expression of fibronectin isoforms in human breast tissue: production of extra domain A+/extra domain B+ by cancer cells and extra domain A+ by stromal cell. Jpn. J. Cancer Res. **90:**320–325.
36. **McCarty, J. H., R. A. Monahan-Earley, L. F. Brown, M. Keller, H. Gerhardt, K. Rubin, M. Shani, H. F. Dvorak, H. Wolburg, B. L. Bader, A. M. Dvorak, and R. O. Hynes.** 2002. Defective associations between blood vessels and brain parenchyma lead to cerebral hemorrhage in mice lacking αv integrins. Mol. Cell. Biol. **22:**7667–7677.
37. **Morikawa, S., P. Baluk, T. Kaidoh, A. Haskell, R. K. Jain, and D. M. McDonald.** 2002. Abnormalities in pericytes on blood vessels and endothelial sprouts in tumors. Am. J. Pathol. **160:**985–1000.
38. **Muro, A. F., A. K. Chauhan, S. Gajovic, A. Iaconcig, F. Porro, G. Stanta, and F. E. Baralle.** 2003. Regulated splicing of the fibronectin EDA exon is essential for proper skin wound healing and normal lifespan. J. Cell Biol. **162:**149–160.
39. **Ni, H., P. S. Yuen, J. M. Papalia, J. E. Trevithick, T. Sakai, R. Fassler, R. O. Hynes, and D. D. Wagner.** 2003. Plasma fibronectin promotes thrombus growth and stability in injured arterioles. Proc. Natl. Acad. Sci. USA **100:**2415–2419.
40. **Ohnishi, T., S. Hiraga, S. Izumoto, H. Matsumura, Y. Kanemura, N. Arita, and T. Hayakawa.** 1998. Role of fibronectin-stimulated tumor cell migration in glioma invasion in vivo: clinical significance of fibronectin and fibronectin receptor expressed in human glioma tissues. Clin. Exp. Metastasis **16:**729–741.
41. **Oyama, F., S. Hirohashi, Y. Shimosato, K. Titani, and K. Sekiguchi.** 1989. Deregulation of alternative splicing of fibronectin pre-mRNA in malignant human liver tumors. J. Biol. Chem. **264:**10331–10334.
42. **Oyama, F., S. Hirohashi, Y. Shimosato, K. Titani, and K. Sekiguchi.** 1990. Oncodevelopmental regulation of the alternative splicing of fibronectin premessenger RNA in human lung tissues. Cancer Res. **50:**1075–1078.
43. **Peters, J. H., G. E. Chen, and R. O. Hynes.** 1996. Fibronectin isoform distribution in the mouse. II. Differential distribution of the alternatively spliced EIIIB, EIIIA, and V segments in the adult mouse. Cell Adhes. Commun. **4:**127–148.
44. **Peters, J. H., and R. O. Hynes.** 1996. Fibronectin isoform distribution in the mouse. I. The alternatively spliced EIIIB, EIIIA, and V segments show widespread codistribution in the developing mouse embryo. Cell Adhes. Commun. **4:**103–125.
45. **Peters, J. H., J. E. Trevithick, P. Johnson, and R. O. Hynes.** 1995. Expression of the alternatively spliced EIIIB segment of fibronectin. Cell Adhes. Commun. **3:**67–89.
46. **Pujuguet, P., A. Hammann, M. Moutet, J. L. Samuel, F. Martin, and M. Martin.** 1996. Expression of fibronectin ED-A+ and ED-B+ isoforms by human and experimental colorectal cancer. Contribution of cancer cells and tumor-associated myofibroblasts. Am. J. Pathol. **148:**579–592.
47. **Ramaswamy, S., K. N. Ross, E. S. Lander, and T. R. Golub.** 2003. A molecular signature of metastasis in primary solid tumors. Nat. Genet. **33:**49–54.
48. **Rodriguez-Manzaneque, J. C., T. F. Lane, M. A. Ortega, R. O. Hynes, J.**

Lawler, and M. L. Iruela-Arispe. 2001. Thrombospondin-1 suppresses spontaneous tumor growth and inhibits activation of matrix metalloproteinase-9 and mobilization of vascular endothelial growth factor. Proc. Natl. Acad. Sci. USA **98:**12485–12490.

49. **Rohan, R. M., A. Fernandez, T. Udagawa, J. Yuan, and R. J. D'Amato.** 2000. Genetic heterogeneity of angiogenesis in mice. FASEB J. **14:**871–876.
50. **Ruchoux, M. M., V. Domenga, P. Brulin, J. Maciazek, S. Limol, E. Tournier-Lasserve, and A. Joutel.** 2003. Transgenic mice expressing mutant Notch3 develop vascular alterations characteristic of cerebral autosomal dominant arteriopathy with subcortical infarcts and leukoencephalopathy. Am. J. Pathol. **162:**329–342.
51. **Ruoslahti, E.** 2002. Specialization of tumour vasculature. Nat. Rev. Cancer **2:**83–90.
52. **Scarpino, S., A. Stoppacciaro, C. Pellegrini, A. Marzullo, L. Zardi, F. Tartaglia, G. Viale, and L. P. Ruco.** 1999. Expression of EDA/EDB isoforms of fibronectin in papillary carcinoma of the thyroid. J. Pathol. **188:**163–167.
53. **Serini, G., M. L. Bochaton-Piallat, P. Ropraz, A. Geinoz, L. Borsi, L. Zardi, and G. Gabbiani.** 1998. The fibronectin domain ED-A is crucial for myofibroblastic phenotype induction by transforming growth factor-β1. J. Cell Biol. **142:**873–881.
54. **Smith, L. E., E. Wesolowski, A. McLellan, S. K. Kostyk, R. D'Amato, R. Sullivan, and P. A. D'Amore.** 1994. Oxygen-induced retinopathy in the mouse. Investig. Ophthalmol. Vis. Sci. *35*:101–111.
55. **Takasaki, I., A. V. Chobanian, W. S. Mamuya, and P. Brecher.** 1992. Hypertension induces alternatively spliced forms of fibronectin in rat aorta. Hypertension **20:**20–25.
56. **Takasaki, I., A. V. Chobanian, R. Sarzani, and P. Brecher.** 1990. Effect of hypertension on fibronectin expression in the rat aorta. J. Biol. Chem. **265:**21935–21939.
57. **Tan, M. H., Z. Sun, S. L. Opitz, T. E. Schmidt, J. H. Peters, and E. L. George.** 2004. Deletion of the alternatively spliced fibronectin EIIIA domain in mice reduces atherosclerosis. Blood **104:**11–18.
58. **Tarli, L., E. Balza, F. Viti, L. Borsi, P. Castellani, D. Berndorff, L. Dinkelborg, D. Neri, and L. Zardi.** 1999. A high-affinity human antibody that targets tumoral blood vessels. Blood **94:**192–198.